Supporting Information for

A pH-Stable Dynamic DNA Nanomachine with Controllable Conformational Switching

Lixuan Lin, [a, b] Kaiyi Liang, [c] Xiuli Gao, [d] Jiang Li, [e] Linjie Guo, [*, e] Kai Jiao, [*, e] Lihua Wang, [e, f]

[a] CAS Key Laboratory of Interfacial Physics and Technology, ShanghaiInstitute of Applied PhysicsChinese Academy of SciencesShanghai 201800, China

[b] University of Chinese Academy of SciencesBeijing 100049, China

[c] Radiology Department of Jiading District Central Hospital Affiliated Shanghai University of Medicine &Health Sciences, Shanghai 201800, China

[d] State Key Laboratory of Transducer Technology, Shanghai Institute of Microsystem and Information Technology, Chinese Academy of Sciences, Shanghai 200050, China

[e] Institute of Materiobiology, College of Sciences, Shanghai University, Shanghai 200444, China

[f] Shanghai Collaborative Innovation Center of Intelligent Sensing Chip Technology, Shanghai University, Shanghai 200444, China

* E-mail: kjiao@shu.edu.cn, guolinjie@shu.edu.cn

Materials

All chemicals and solvents, including artificial lysosomal fluid (ALF), were obtained from commercial suppliers and used without further purification. DNA oligonucleotides were purchased from Sangon Biotech (Shanghai) Co., Ltd. and purified by high-performance liquid chromatography (HPLC). All oligonucleotide sequences are listed in Table S1.

The 1× TAE (Mg^{2+}) buffer was prepared according to the standard formulation (40 mM Tris, 20 mM acetic acid, 2 mM EDTA, and 12.5 mM magnesium acetate) and adjusted to pH 8.0 with acetic acid for use in the assembly of 6H-NNM. Buffers of other pH values were prepared by adjusting the solution with NaOH or HCl as appropriate; specifically, buffers at pH 5-7 were titrated with HCl, whereas buffers at pH 9-11 were adjusted using NaOH.

Methods

Preparation of 6H-NNM

To assemble the 6H-NNM structure, the constituent single-stranded DNA sequences (listed in Table S1) were combined in 1× TAE (Mg^{2+}) buffer. The mixture was then subjected to a gradual annealing process, cooling from 95 °C to ambient temperature over a 12-hour period using a water bath insulated within a 1 L foam container.

AFM Imaging

For atomic force microscopy (AFM) analysis, 10 μL of the DNA sample (20 nM in synthetic buffer) was deposited onto mica that had been pretreated with APTES for 1.5 minutes and subsequently washed with Milli-Q water. The sample was allowed to adsorb on the surface for 5 minutes before imaging. AFM measurements were conducted on a Bruker instrument using Fluid+ probes (Veeco Inc., USA).

Height profiles were extracted from the AFM topographic images. Individual, well-isolated particles were selected for cross-sectional analysis. For each particle, a line profile was drawn perpendicular to its long axis using the instrument's analysis software (Bruker NanoScope Analysis). The height value was taken as the vertical

distance between the substrate baseline and the top of the particle.

Native gel electrophoresis

Native polyacrylamide gel electrophoresis (PAGE) was employed to assess the assembly states of the DNA structures. Samples obtained after annealing were loaded onto freshly prepared 6% native polyacrylamide gels and separated in TAE-Mg^{2+} running buffer composed of 40 mM Tris-HCl, 20 mM acetic acid, 2 mM EDTA, and 12.5 mM magnesium acetate. Electrophoresis was performed in a Bio-Rad gel system at a constant voltage of 100 V for 2 h at room temperature. Following separation, gels were stained with Gel Red according to the manufacturer's instructions and imaged using a standard gel documentation system to visualize the DNA bands.

Fluorescence kinetic curve fitting analysis

To obtain kinetic parameters that specifically reflect the conformational switching efficiency independent of pH-induced variations in fluorophore brightness, all raw fluorescence trajectories were first normalized and subsequently fitted with a reversible kinetic model.

1. Fluorescence intensity normalization

The fluorescence intensity of the closed-state 6H-NNM (labeled with both Alexa Fluor 488 and the BHQ1 quencher) was defined as the baseline F_{min}. The intensity of a control structure identical to 6H-NNM but lacking the BHQ1 quencher (labeled only with Alexa Fluor 488) was taken as the fully unquenched signal F_{max}. For each raw fluorescence intensity f(t), the normalized fluorescence F(t) was calculated as:

$$F(t) = \frac{f(t) - Fmin}{Fmax - Fmin}$$

This normalization corrects for any pH-dependent changes in fluorophore quantum yield, ensuring that the resulting trajectories report exclusively on quenching efficiency changes due to strand-displacement-driven conformational switching.

2. Kinetic fitting of normalized trajectories

The normalized fluorescence–time data F(t) from forward (unlocking) and reverse (relocking) reactions were analyzed using a reversible second-order kinetic model. The signal was fitted to the analytical solution:

$$F(t) = F_{eq} + (F_0 - F_{eq})e^{-(k_1 + k_2)t}$$

where F_0 is the initial fluorescence, F_{eq} is the equilibrium fluorescence, and k_1 and k_2 represent the forward and reverse apparent rate constants, respectively. Initial parameter estimates were obtained from the first and last data points of each trajectory. Non-linear least-squares fitting was performed using the Levenberg–Marquardt algorithm implemented in SciPy's curve_fit. Goodness-of-fit was evaluated by the coefficient of determination $\boldsymbol{R^2}$:

$$R^2 = 1 - \frac{\sum (F_{exp} - F_{fit})^2}{\sum (F_{exp} - \bar{F}_{exp})^2}$$

To compare dynamic behaviors, the fluorescence enhancement level $\boldsymbol{F_{inf}}$ was calculated using the following equation:

$$F_{inf} = F_{eq} - F_0$$

and the area under the fitted fluorescence curve (***AUC***) was determined using Simpson's rule.

To quantify reaction kinetics, the apparent rate constant $\boldsymbol{k_{obs}}$ and half-life $\boldsymbol{t_{half}}$ were calculated from the fitted parameters according to:

$$k_{obs} = k_1 + k_2$$

$$t_{half} = \frac{ln2}{k_1 + k_2}$$

For each sample, both forward and reverse reactions were analyzed, and the conformational conversion ***Recovery Ratio*** was calculated as follows:

$$Recovery\ Ratio = \frac{F_{0\_Reverse} - F_{eq\_Reverse}}{F_{0\_Reverse} \times \left(1 - \frac{F_{0_{Forward}}}{F_{eq_{Forward}}}\right)}$$

All custom scripts used for kinetic analysis in this study were written in Python (version 3). The full analysis pipeline is provided as a standalone script kinetics_analysis.py, which performs batch fitting of forward and reverse fluorescence–time datasets using a reversible second-order kinetic model. The script implements

nonlinear least-squares fitting (SciPy curve_fit) of the function mentioned above and automatically calculates a series of kinetic parameters. The script further exports dense fitted curves for plotting, reaction-recovery metrics, and a consolidated results table for all samples.

The Python script and usage instructions are included in the Supplementary Information, and are directly executable in a standard Python virtual environment with NumPy, SciPy, Matplotlib, and Pandas installed.

Supporting figures

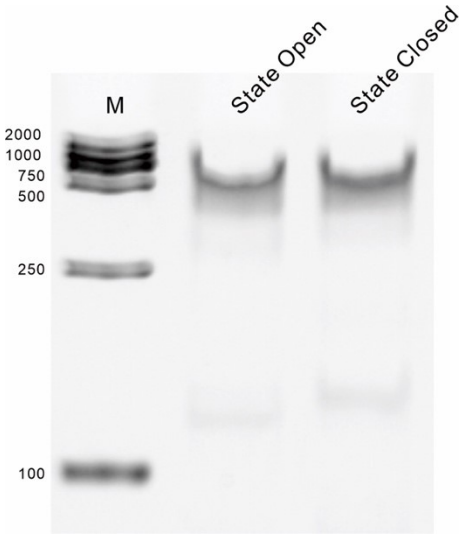

Figure S1. Native PAGE analysis of 6H-NNM in the closed and open states. M：DL 2000 DNA ladder.

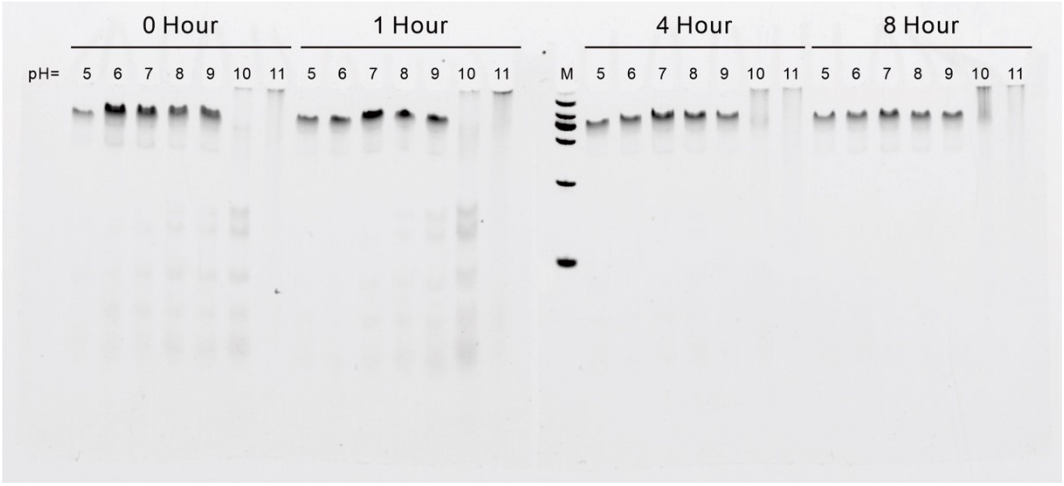

Figure S2. Native PAGE analysis of 6H-NNM samples incubated at room temperature for 0, 1, 4, and 8 h under different pH conditions (pH=5–11). M：DL 2000 DNA ladder.

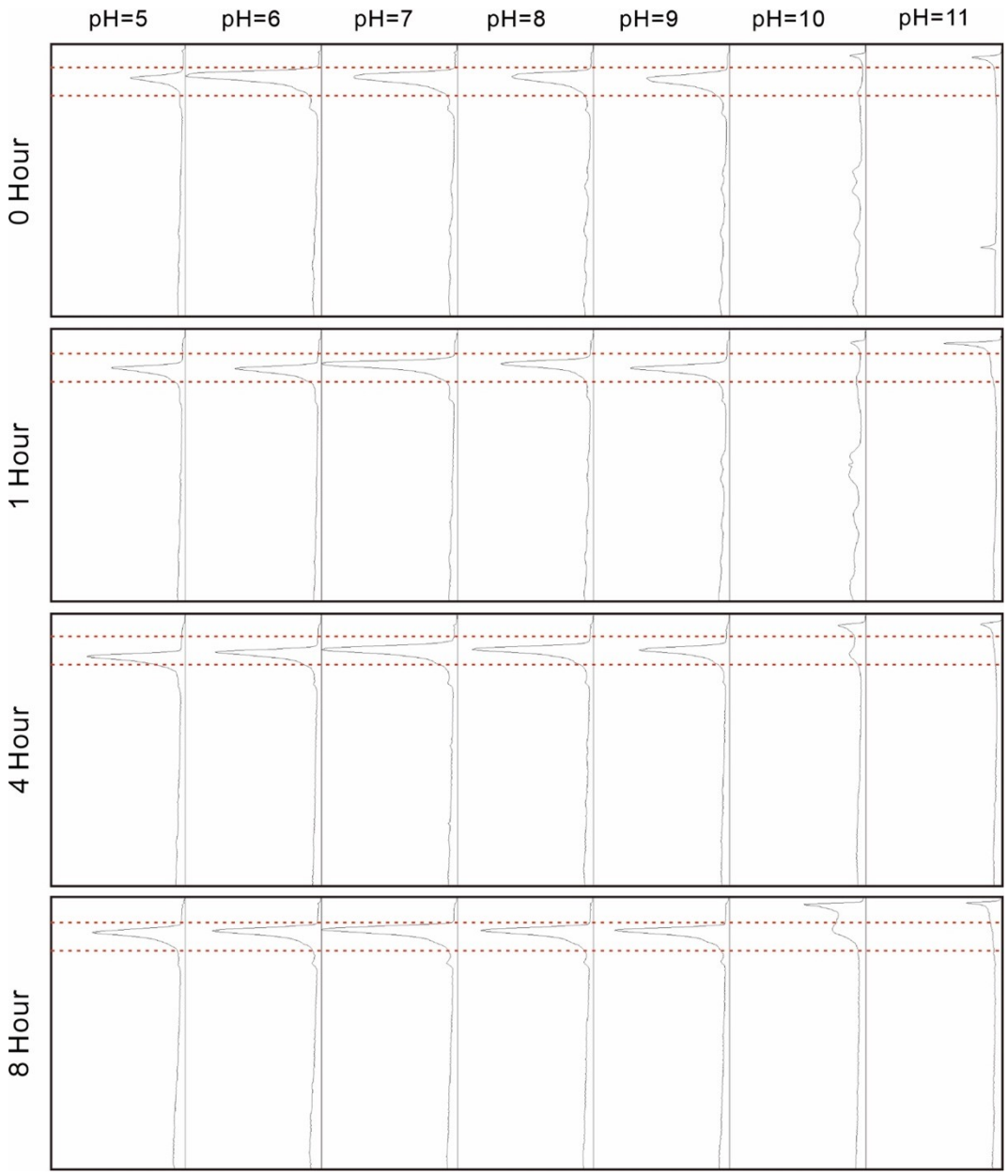

Figure S3. Densitometric analysis of gel images in figures S2 showing the relative band intensities in each lane, reflecting differences in structural integrity over time.

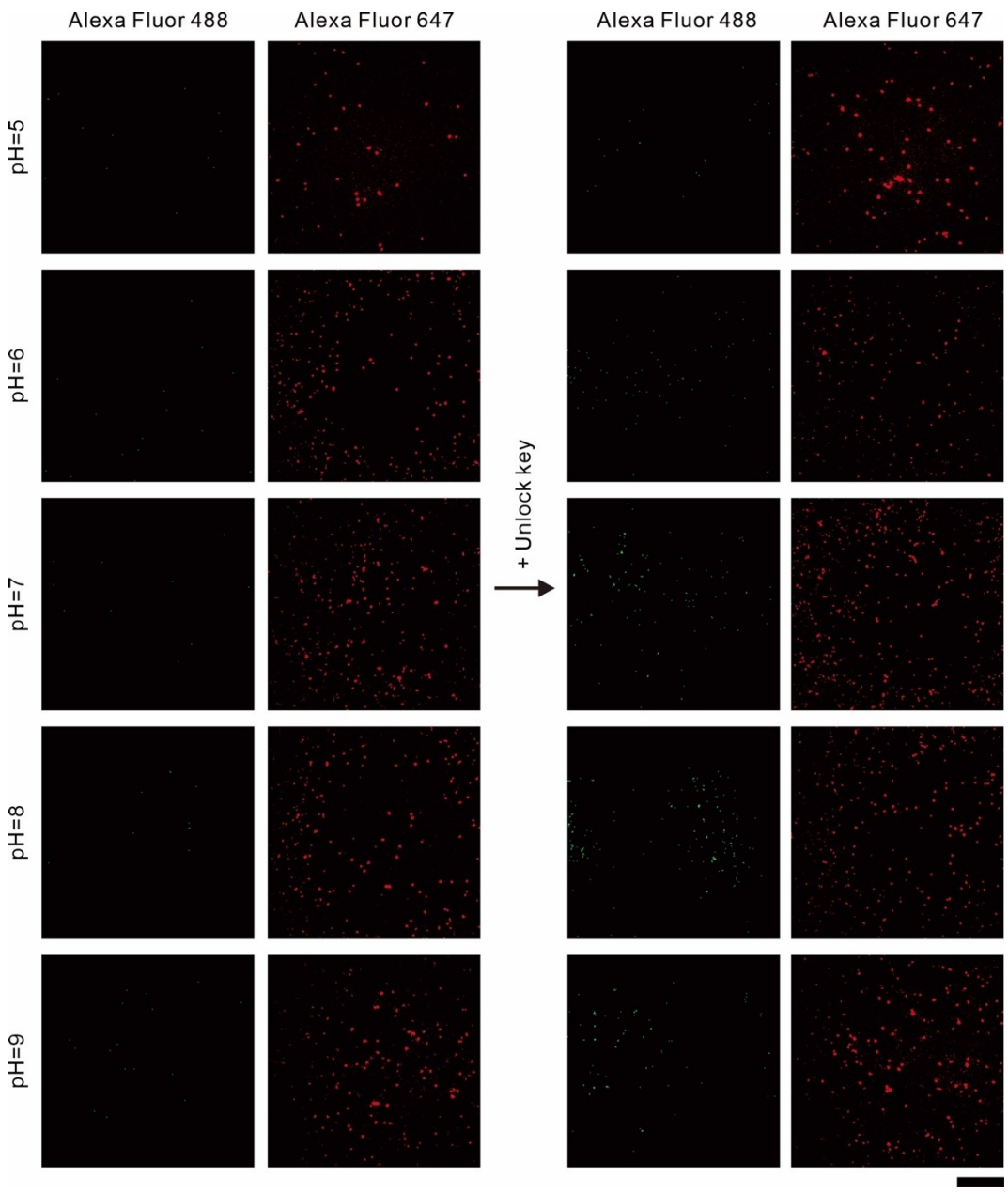

Figure S4. Full field of view images from single molecule fluorescence imaging of 6H-NNM switching events at pH 5–9. Scale bar, 10 μm.

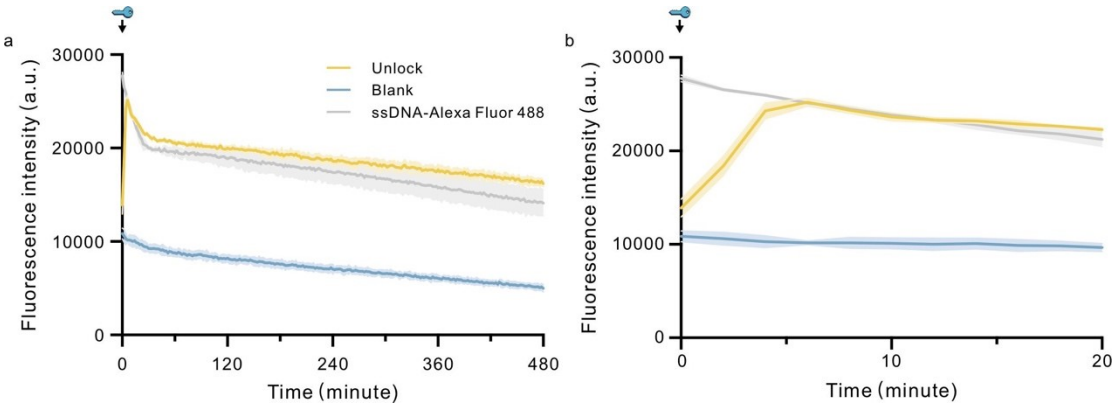

Figure S5. Characterization of 6H-NNM switching and fluorophore stability in artificial lysosomal fluid (ALF). (a) Long-term fluorescence trajectories over 8 h for: (i) closed-state 6H-NNM (Blank, no key added); (ii) 6H-NNM after Unlock key addition (Unlock); and (iii) a control single-stranded DNA labeled with Alexa Fluor 488 (ssDNA-Alexa Fluor 488). (b) Real-time fluorescence monitoring during the first 20 min immediately after Unlock key addition. Data are mean ± s.d. (n = 3 technical replicates).

The closed-state nanomachine maintained low fluorescence, confirming structural integrity. Upon Unlock key addition, the rapid fluorescence increases confirmed successful switching. The subsequent fast decay in fluorescence for both the unlocked nanomachine and the ssDNA control, followed by parallel slower decay phases, indicates that the signal reduction is primarily due to photophysical instability of the fluorophore in the ALF environment, rather than structural destabilization of 6H-NNM.

Supporting tables

Table S1. DNA sequences used for the assembly of the 6H-NNM.

Name	Sequence（5’-3’）
6H-NNM-1	CAGTTGACTGCTAGTACCTGAGCACTGAATGCGATGTAGAAG TAGCTCTGCTCCATC
6H-NNM-2	CGACTTGATGGAGCAGACCTATCGTCAC
6H-NNM-3	AGGCAGATACGAAGAGCGCCGGGCTGTCGTAGATAGTTCTCG CACGACGCTAGACAC
6H-NNM-4	GCAGTCAACTG
6H-NNM-5	CGGTACGTGACGATAGGACACATCAGATGTCTTAGGAGAGGT CACAGTAACCTTCGACAATCT
6H-NNM-6	AGATTGTCGAACGTATCTGCCT
6H-NNM-7-Alexa 488	GAACTATGACATCTGATGTGTGCTACTTGGCTGCTTAGAC
6H-NNM-8	CGCTCTTGGTTACTGTGACCTGTGCTCAGCCGCTTTGAAT
6H-NNM-9	GCATTCACTCCTAACTACGAC
6H-NNM-10	TCTAGCGTGTCTAGCGT
6H-NNM-11	TGTCCGTGCAACCGATCAATCC
6H-NNM-12	GCCTAGCGATCCAATGGAACGACCGTATTGCTGAGGTGAGTG TATGTATCACTTGCACGGACA
6H-NNM-13-BHQ1	CTGTACCGTTG
6H-NNM-14	GGATTGATCGGATGCCAGACGCATCGGATTCGATGAGCCTAC TCGACCAACTCAACG
6H-NNM-15	GGCAATGTCCACCATTGGATCG
6H-NNM-16	CAACGGTACAGGGCAGCCTCCAACCTTGTAACCAGCGGCATA ACGCTGGACATTGCC
6H-NNM-17	GGAGGCGTGCGACTGGCATGTGATACATACACTGGTTGGA

6H-NNM-18	GGATGAGCCCGGGGCTCATGCAATACGGTCGTTGCGTTAT
6H-NNM-19	GTTACAACACCTCACGAATCC
6H-NNM-20	GCACCACGTTGAGTTGG

Table S2. Sequences of the Unlock and Relock keys used for conformational switching of 6H-NNM.

Name	Sequence（5’-3’）
Unlock key 1	ATCATGTCTAGGCAGCC
Unlock key 2	GGTCTATTCACAGCGGC
Relock key 1	GGCTGCCTAGACATGAT
Relock key 2	GCCGCTGTGAATAGACC

Table S3. Composition of the artificial lysosomal fluid (ALF).

Component	**Concentration（g/L）**
Sodium chloride	3.21
Dibasic sodium phosphate	0.071
Sodium citrate dihydrate	0.077
Sodium tartrate dihydrate	0.09
Sodium lactate	0.085
Sodium pyruvate	0.086
Calcium chloride Dihydrate	0.128
Glycine	0.059
Sodium hydroxide	6
Magnesium chloride	0.05
Sodium sulphate	0.039
Citric acid	20.8